Sea Surface Temperature–Precipitation Relationship in Different Reanalyses

ARUN KUMAR

Climate Prediction Center, NOAA/NWS/NCEP, College Park, Maryland

LI ZHANG

Climate Prediction Center, NOAA/NWS/NCEP, College Park, Maryland, and Wyle Science, Technology, and Engineering, McLean, Virginia

WANQIU WANG

Climate Prediction Center, NOAA/NWS/NCEP, College Park, Maryland

(Manuscript received 2 August 2012, in final form 22 November 2012)

ABSTRACT

The focus of this investigation is how the relationship at intraseasonal time scales between sea surface temperature and precipitation (SST–*P*) varies among different reanalyses. The motivation for this work was spurred by a recent report that documented that the SST–*P* relationship in Climate Forecast System Reanalysis (CFSR) was much closer to that in the observation than it was for the older generation of reanalyses [i.e., NCEP–NCAR reanalysis (R1) and NCEP–Department of Energy (DOE) reanalysis (R2)]. Further, the reason was attributed either to the fact that the CFSR is a partially coupled reanalysis, while R1 and R2 are atmospheric-alone reanalyses, or that R1 and R2 use the observed weekly-averaged SST.

The authors repeated the comparison of the SST–*P* relationship among R1, R2, and CFSR, as well as two recent generations of atmosphere-alone reanalyses, the Modern-Era Retrospective Analysis for Research and Applications (MERRA) and the ECMWF Re-Analysis Interim (ERA-Interim). The results clearly demonstrate that the differences in the SST–*P* relationship at intraseasonal time scales across different reanalyses are not due to whether the reanalysis system is coupled or atmosphere alone, but are due to the specification of different SSTs. The SST–*P* relationship in different reanalyses, when computed against a single SST for the benchmark, demonstrates a relationship that is common across all of the reanalyses and observations.

1. Introduction

Results have shown that correct representation of ocean–atmosphere interaction in models is important for simulating certain aspects of climate such as the organization and propagation of intraseasonal variability (Flatau et al. 1997; Seo et al. 2007). Another such feature is the precipitation variability and its relationship with underlying sea surface temperatures (SSTs; Pegion and Kirtman 2008; Wu et al. 2008; Chen et al. 2012). Precipitation and SST at intraseasonal time scales are characterized by lead–lag relationships with the SST leading precipitation when the atmosphere is forced by SSTs and with the precipitation leading SST when ocean variability is driven by the atmospheric circulation (Wu et al. 2008).

At longer time scales, the SST–precipitation (SST–*P*) relationship in observations varies markedly with oceanic regions where correlation is highly positive (e.g., in the tropical eastern Pacific) versus regions where correlation is either near zero or is even slightly negative (e.g., over the western Pacific and Indian Oceans). The former corresponds to regions where slow ocean variability controls the atmospheric variability, and this relationship is well simulated with atmosphere-only models forced with observed SSTs [the so-called Atmospheric Model Intercomparison Project (AMIP) simulations]. For the latter, it is generally argued that the negative SST–*P* correlation is because the atmospheric variability is the controlling mechanism for the SST variability (Wu et al. 2006). For this case, AMIP simulations, where evolution of SSTs is specified and may not be consistent

Corresponding author address: Arun Kumar, 5830 University Research Court, Room 3000, College Park, MD 20740.
E-mail: arun.kumar@noaa.gov

DOI: 10.1175/MWR-D-12-00214.1

with air–sea fluxes, by design cannot replicate the observed SST–*P* relationship (Kumar and Hoerling 1998). Indeed, the observed SST–*P* relationship is generally better reproduced in coupled model simulations where atmospheric variability can influence the evolution of underlying SSTs. On the other hand, it remains controversial as to how the feedback of SST evolution adds to improvements in different aspects of atmospheric variability on various time scales (Saravanan 1998; Jha and Kumar 2009).

Another area where correct representation of the ocean–atmosphere interaction may have a role is the analysis of the earth system, for example, the reanalysis efforts. To date, reanalyses, for example, the National Centers for Environmental Prediction–National Center for Atmospheric Research (NCEP–NCAR) reanalysis (R1; Kalnay et al. 1996) and NCEP–Department of Energy (DOE) reanalysis (R2; Kanamitsu et al. 2002), are generally run in an uncoupled mode where SSTs are specified. This paradigm is also followed in the two recent reanalyses efforts: the Modern-Era Retrospective Analysis for Research and Applications (MERRA; Rienecker et al. 2011) and the European Centre for Medium-Range Weather Forecasts (ECMWF) Re-Analysis Interim (ERA-Interim; Dee et al. 2011). One exception has been the Climate Forecast System Reanalysis (CFSR; Saha et al. 2010) that was done in partially coupled mode in which the analysis of oceanic and atmospheric components are done separately, while the 6-h guess forecast is made based on a coupled model.

An investigation of the CFSR indicated that the SST–*P* correlation was much better simulated when compared to the older generation of reanalyses (R1 and R2). The inferior representation of SST–*P* correlation in R1 and R2 was attributed to either the lack of coupling in these two reanalyses or their use of weekly-averaged SSTs (Saha et al. 2010). In this paper we extend previous investigation 1) to verify if the same conclusion holds for the comparison of CFSR against its more contemporary peers (i.e., MERRA and ERA-Interim); 2) if not, to determine the reasons for the result in Saha et al. (2010); and 3) if the SST–*P* relationship is the same between the CFSR and other atmosphere-alone reanalyses, to explain how the result about the importance of coupled ocean–atmosphere evolution can be reconciled between reanalyses and model-free simulations.

2. Data and analysis procedure

The investigation is based on data covering 1997–2008. The Global Precipitation Climatology Project (GPCP; Huffman et al. 2001) daily precipitation and the National Climatic Data Center (NCDC) daily SST (Reynolds et al. 2007) are used for observations. The reanalysis daily precipitation and SST are from the three most recent reanalyses—CFSR, MERRA, and ERA-Interim. In addition, two older reanalyses, R1 (Kalnay et al. 1996) and R2 (Kanamitsu et al. 2002) used in Saha et al. (2010), are also included.

The daily precipitation and SST were first interpolated to a common 2.5° latitude × 2.5° longitude grid. Daily anomalies were then computed as the departure from seasonal climatology defined as the annual mean plus the first four harmonics over 1997–2008. To focus on the intraseasonal variability, we use intraseasonal anomalies obtained by applying 20–100-day bandpass filtering to the raw daily-mean anomalies. All results in this paper are for the average over the tropical western Pacific (10°S–10°N, 130°–150°E) for the boreal winter (November–April) when the intraseasonal oscillation is strongest and most frequent (Woolnough et al. 2000), as in Saha et al. (2010).

For all of the reanalyses, except CFSR, the evolution of SST is prescribed. The MERRA SST was derived from the weekly optimum interpolation SST, version 2 (OISST v2) of Reynolds et al. (2002), linearly interpolated to each model time step (Rienecker et al. 2011). ERA-Interim used a succession of different SST data products (Dee et al. 2011), including the NCEP two-dimensional variational data assimilation (2D-Var) until June 2001, the OISST v2 of Reynolds et al. (2002), and the NCEP real-time global (RTG) daily SST analysis starting January 2002. Both R1 and R2 used the NCEP operational SST analysis produced based on observations of the previous 7 days. For the CFSR, the 6-hourly predicted SST was strongly relaxed to the NCDC daily SST analysis (Reynolds et al. 2007). We should note that a distinction is made between the NCDC SST (which will be used later as the benchmark SST) and reanalyses' SSTs, and two factors contribute toward this: 1) first of all and as mentioned above, different reanalyses do not use NCDC SST to begin with, and 2) for reanalyses, the SST is first taken from one of the available observed SST analyses; it is then interpolated to assimilation systems' time and spatial resolution; and at the final stage is reassembled as a daily mean value of ''reanalysis'' SST product. Because of the processing that is built in going from the ''observed'' to the ''reanalysis'' SST, input-observed SST need not be identical to the reanalysis SST (Taylor et al. 2000).

3. SST–*P* relationship among different reanalyses

An assessment similar to that in Saha et al. (2010) is shown in Fig. 1 to compare the lead–lag relationships between filtered SST–*P* among observations and

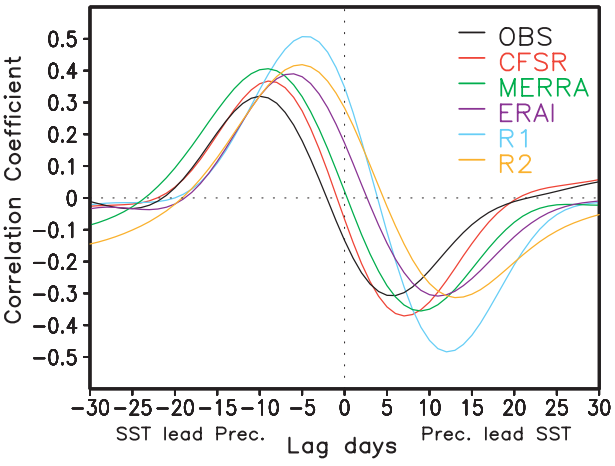

FIG. 1. Lead–lag SST–*P* correlations for various reanalyses and for observations over the tropical western Pacific (averaged over 10°S–10°N, 130°–150°E). Negative (positive) lag in days on the *x* axis indicates by which the SST leads (lags) the precipitation. Computational details are given in section 2, and for each of the reanalyses, respective SSTs were used.

reanalyses. For observations (black curve), positive correlation gradually increases with lead time for SST leading precipitation until the correlation reaches the maximum at the lead of 10 days, indicating that prior to precipitation reaching its peak, SSTs have a warming tendency. Further, once precipitation reaches its peak, SSTs have a decreasing tendency afterward resulting in a negative SST–*P* correlation (for precipitation leading SST variability) with the minimum value at the lead time of 6 days.

The positive SST–*P* correlation at negative lags corresponds to the situation where the ocean surface condition is influencing atmospheric changes. The lag time of the maximum SST–*P* provides an estimate of the time that it takes for the atmosphere to respond to SST anomalies. The negative observed SST–*P* correlation at positive lags is consistent with the concept of atmospheric variability driving the ocean through changes in surface heat fluxes, which directly affect ocean surface heat balance, and momentum fluxes, which affect the ocean heat balance through dynamic advection and mixing. For example, a decrease (increase) in precipitation, corresponding to clear (cloudy) sky conditions and increase (decrease) shortwave flux at surface, results in heating (cooling) of oceanic mixed layer and an increase (decrease) in SSTs. The feedback loop described, however, may be an oversimplification as other components of surface heat fluxes, for example, latent and sensible heat, as well as changes in ocean mixing due to changes in surface winds in response to precipitation variability, may also play a role.

The correlation in Fig. 1 for reanalyses is calculated using SSTs from the respective reanalysis products. By and large the observed SST–*P* lead–lag correlation is replicated and the correlation is positive (negative) when SST leads (lags) precipitation. However, some important differences exist. One of the largest differences is between the CFSR and older generation of reanalyses, R1 and R2. While the observed relationship is well simulated in CFSR with a positive SST–*P* correlation peak around day –9, the peak in positive correlation is at −4 (−5) days in R1 (R2). This discrepancy between CFSR and R1 and R2 was noted in Saha et al. (2010). Further, since CFSR is a partially coupled ocean–atmosphere reanalysis while SSTs are specified in R1 and R2, it led to the conclusion that the better representation of the SST–*P* relationship in the CFSR was either due to the inclusion of the coupled ocean–atmosphere evolution or the use of weekly SST in R1 and R2.

A comparison of the SST–*P* relationship between CFSR and its more recent peers—MERRA and ERA-Interim—in which SSTs are also specified, leads to a different impression. The SST—*P* relationship in MERRA is very similar to that in observations (or in the CFSR), while for the ERA-Interim, the peak in positive SST–*P* correlation is somewhere in between the CFSR and R1 and R2. This is irrespective of the fact that both MERRA and ERA-Interim are atmosphere-alone reanalyses.

A better simulation of SST–*P* relationship in MERRA and ERA-Interim compared to that in R1 and R2 may be due to the former being more advanced models and data assimilation systems than earlier generation of reanalyses, and it is conceivable that advances in ingesting observational data may compensate for them being atmosphere-alone assimilation systems. However, there may also be an alternate explanation for variations in the SST–*P* relationship.

The SST–*P* relationship among different reanalyses in Fig. 1 is based on SST and precipitation data from the respective reanalyses. It is possible that even though precipitation variability among different reanalyses may be similar, variations in the SST–*P* relationship are merely due to the use of different reanalysis SSTs in the lead–lag analysis. This possibility can be eliminated if the lead–lag correlation between precipitation and SST is computed against a single reference SST dataset.

Using NCDC SST analysis as the reference, the SST–*P* relationship for all five reanalyses is recomputed and is shown in Fig. 2. With the use of single SST dataset, there is a remarkable similarity in the SST–*P* lead–lag relationship among all of the reanalyses and the observation, and further, the discrepancy noted in Fig. 1 disappears. This indicates that the differences in the SST–*P* relationship are indeed related to how the SSTs in reanalyses differed. This possibility is also supported by the fact that the time difference between the SST–*P* correlation

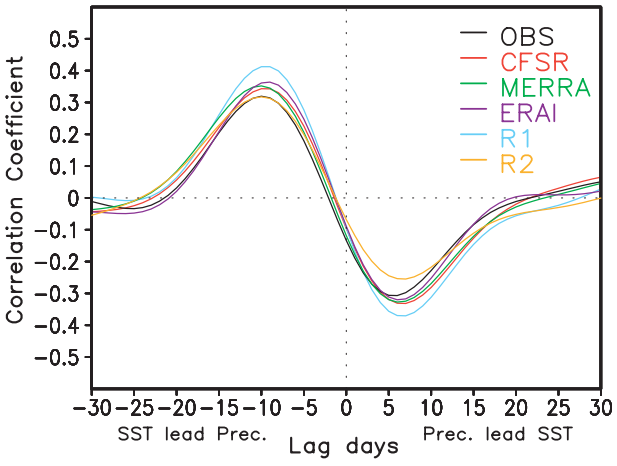

FIG. 2. As in Fig. 1, but the lead–lag SST–*P* correlations for different reanalyses are computed with NCDC SST as the benchmark.

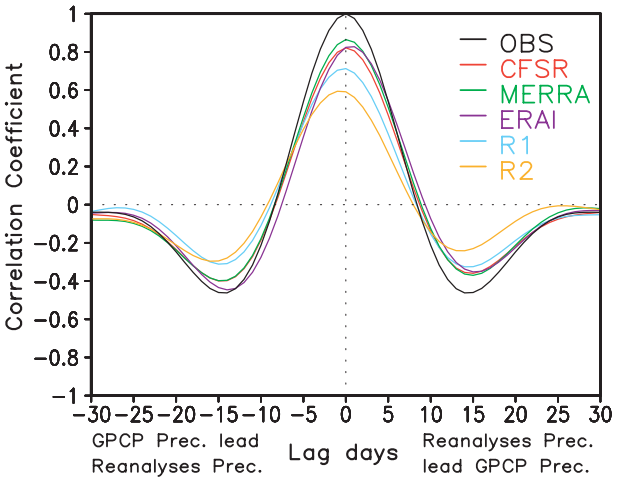

FIG. 3. Lead–lag correlations between precipitation from different reanalyses and GPCP-observed precipitation. Negative (positive) lag in days on the *x* axis indicates days by which the GPCP precipitation leads (lags) the reanalysis precipitation.

maximum (at negative lag) and minimum (at positive lag) is about the same for all reanalyses and the observation (Table 1), and could happen if the precipitation variability for various reanalyses remains the same but the SSTs' different reanalyses are phase shifted due to different specifications.

To further confirm that differences in the SST–*P* relationship in Fig. 1 were indeed due to variations in SST among different reanalyses, we performed two additional sets of computations. We first computed the lead–lag correlation between precipitation from different reanalyses and precipitation from the GPCP (as an independent estimate of the observed precipitation). The result shown in Fig. 3 indicates that with GPCP precipitation as the benchmark, temporal variability in precipitation in other reanalyses has a similar lead–lag behavior. The correlation for all reanalyses peaks at around lag zero and indicates that all reanalyses replicate the temporal phase of the observed intraseasonal variability in precipitation well. The primary difference among various reanalyses is the amplitude of correlation at lag zero, which is less for the earlier generation of reanalyses, while it is similar for the three recent reanalyses.

Using a similar approach we also calculated lead–lag correlation between NCDC SST and SSTs used in different reanalyses (Fig. 4). These results confirm that differences in SSTs among reanalyses exist. For CFSR and MERRA the correlation maximizes at zero lag. For other reanalyses, however, there is a phase shift between reanalyses and NCDC SST, and further, the shift is the largest for R1 and R2. The sequence when the peak in the positive correlation for SST occurs for different reanalyses in Fig. 4 has a good correspondence with differences in the peak of positive SST–*P* correlation in Fig. 1. For example, both for the CFSR and MERRA the peak in positive SST–*P* correlation aligns with that for observation, while the lead–lag SST correlation for the same two reanalyses in Fig. 4 also peaks at lead zero.

TABLE 1. Time difference (days) between maximum positive and minimum negative correlations in Fig. 1.

Dataset	Time diff
Observation	16
CFSR	16
MERRA	18
ERA-Interim	17
R1	16
R2	18

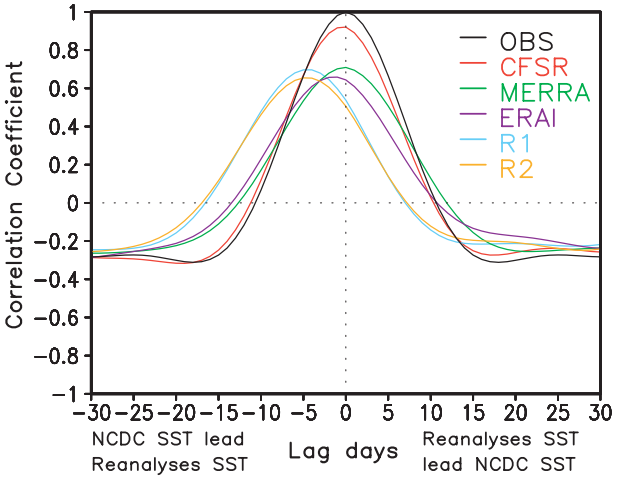

FIG. 4. Lead–lag correlations between SSTs from different reanalyses and the NCDC SST analysis. Negative (positive) lag in days on the *x* axis indicates days by which the NCSC SST leads (lags) SSTs in other reanalyses.

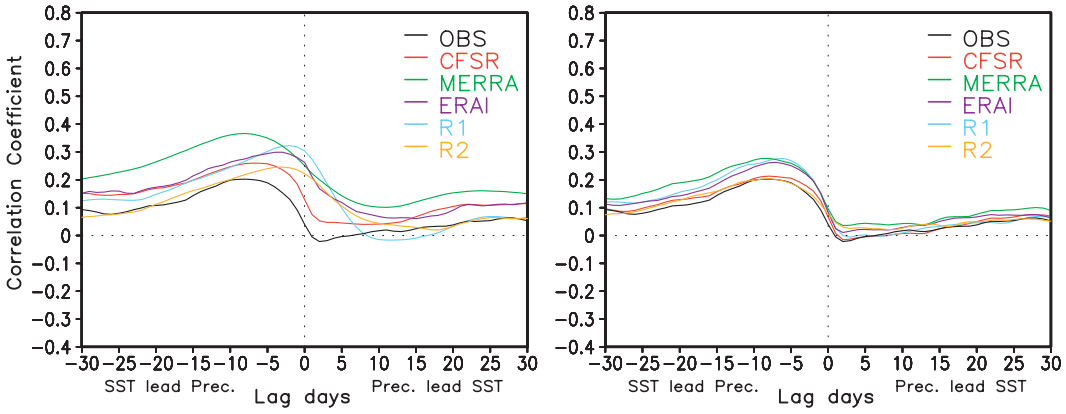

FIG. 5. As in Fig. 1, but for lead–lag correlations for unfiltered data. Lead–lag SST–*P* correlations (left) when respective SSTs were used and (right) when NCDC SST was used as the benchmark.

Similarly, the difference in SST–*P* correlation for R1 and R2 is largest from the observations, which is also the case for SST correlations in Fig. 4.

In one final assessment, Fig. 5 shows the lead–lag correlation for the raw unfiltered data to ascertain that the results shown in Figs. 1–4 were not an artifact of the filtering procedure. By and large, results similar to that for the filtered data also hold for the raw data. Although the amplitude of lead–lag correlations is smaller, SST–*P* correlations for the case in which SSTs are from respective reanalyses (Fig. 5, left) have a different relationship. On the other hand, for NCDC SST as the benchmark, the SST–*P* lead–lag relationship across various reanalyses has the same relationship (Fig. 5, right).

4. Summary and discussion

The results presented here demonstrate that variations in the lead–lag SST–*P* relationship among various reanalyses noted in Saha et al. (2010) were due to the use of different SSTs across the reanalyses and not because CFSR being a partially coupled reanalysis demarcated it from the other atmosphere-alone reanalyses.

A question is whether this result represents an apparent contradiction in that the relationship between precipitation from various reanalyses and a common SST seems to be insensitive to whether the reanalysis is partially coupled or is done in the AMIP mode (where SSTs are specified), while the SST–*P* relationship does differ between CMIP runs, which produce a lead–lag SST–*P* relationship (Inness and Slingo 2003) and AMIP runs that do not (Wu et al. 2002; Chen et al. 2012).

The resolution of this apparent inconsistency may underlie the nature of reanalysis products, and the role of data assimilation whereby atmospheric and satellite observations are ingested at 6-hourly intervals. While SSTs are specified in AMIP simulations as in the atmosphere-only reanalyses, there is a fundamental difference in the evolution of the atmosphere. In AMIP simulations, the atmosphere evolves freely, and although SST variability can influence atmospheric variability (and can produce positive SST–*P* correlations), it cannot be influenced by the atmospheric variability (and cannot produce negative SST–*P* correlations). For the CMIP simulations, the time-evolving atmospheric state is consistent with the ocean surface (as in nature), and one can expect a more realistic SST–*P* relationship in CMIP simulations than that in AMIP simulations. For the atmosphere-only reanalyses, and in contrast to AMIP simulations, if the ingestion of atmospheric observations forces the atmospheric variability (and precipitation) to be close to that observed, and further, if the specified SSTs follow the observed SSTs without a phase shift, then the SST–*P* from the reanalyses would be realistic and closer to that in the CMIP simulations even though the framework of the reanalyses is the same as for the AMIP simulations.

To elaborate further, if the precipitation during the assimilation is controlled by the atmospheric variability [e.g., variability associated with the Madden–Julian oscillation (MJO)], then one may expect that with a reasonable initial analysis of large-scale atmospheric fields, the large-scale atmospheric forcing for precipitation will also be similar, and therefore, may result in similar precipitation among different reanalyses. The control of observed SSTs on the large-scale atmospheric forcing for convection in the atmosphere-alone reanalyses may be included through the ingestion of observations of the atmospheric fields (such as temperature and moisture that determine the atmospheric instability) that are influenced by observed SSTs through the changes in surface fluxes. The assumption about the similarity of large-scale atmospheric variability was demonstrated by Chelliah et al. (2011).

In the assimilation cycle for different reanalyses, the SSTs are continually updated either as a specification in the case of atmosphere-alone reanalyses, or because of nudging toward the observed value as is the case for the CFSR. The combination of the two factors—1) precipitation being largely controlled by the large-scale atmospheric analysis and being similar across different reanalyses (Fig. 3), and 2) observed SST (that, in nature, is the result of coupled ocean–atmosphere interaction) being continually updated during the assimilation cycle—may lead to a situation where different reanalyses preserve the coupled ocean–atmosphere evolution in the observed fields, and therefore, may act as a pseudo-coupled system. So even though a reanalysis is run in the atmosphere-alone (AMIP) mode, continual updates of SST toward the observed value may mimic a realistic SST–*P* behavior similar to that in the observations or in coupled model simulations.

One implication from our study is that the analysis of the relationship between precipitation and ocean surface conditions based on a reanalysis and the SST used in the reanalysis themselves may not be realistic if the specified SSTs are not consistent with the atmospheric state. Use of such a reanalysis product for studying the relationship between the atmospheric variability and SSTs should be based on observed SSTs, and not the SSTs that are reanalysis products. Further, although our result indicates that inconsistent specification of SST does not influence precipitation variability, it might influence air–sea interaction and surface fluxes. For uncoupled atmosphere-only reanalyses, a specification of SSTs without an undesirable time shift is required to provide consistent datasets of atmospheric variables, SSTs, and surface fluxes.

Acknowledgments. We thank Drs. Yan Xue and Zeng-Zhen Hu, and three anonymous reviewers, for constructive comments and suggestions.

REFERENCES

Chelliah, M., W. Ebisuzaki, S. Weaver, and A. Kumar, 2011: Evaluating the tropospheric variability in National Centers for Environmental Prediction's climate forecast system reanalysis. *J. Geophys. Res.,* **116,** D17107, doi:10.1029/2011JD015707.

Chen, M., W. Wang, A. Kumar, H. Wang, and B. Jha, 2012: Ocean surface impacts on the seasonal precipitation over the tropical Indian Ocean. *J. Climate,* **25,** 3566–3582.

Dee, D. P., and Coauthors, 2011: The ERA-Interim reanalysis: Configuration and performance of the data assimilation system. *Quart. J. Roy. Meteor. Soc.,* **137,** 553–597.

Flatau, M., P. J. Flatau, P. Phoebus, and P. P. Niiler, 1997: The feedback between equatorial convection and local radiative and evaporative process: The implication for intraseasonal oscillations. *J. Atmos. Sci.,* **54,** 2373–2386.

Huffman, G. J., R. F. Adler, M. Morrissey, D. Bolvin, S. Curtis, R. Joyce, B. McGavock, and J. Susskind, 2001: Global precipitation at one-degree daily resolution from multi-satellite observations. *J. Hydrometeor.,* **2,** 36–50.

Inness, P. M., and J. M. Slingo, 2003: Simulation of the Madden–Julian Oscillation in a coupled general circulation model. Part I: Comparisons with observations and an atmosphere-only GCM. *J. Climate,* **16,** 345–364.

Jha, B., and A. Kumar, 2009: A comparison of the atmospheric response to ENSO in coupled and uncoupled model simulations. *Mon. Wea. Rev.,* **137,** 479–487.

Kalnay, E., and Coauthors, 1996: The NCEP/NCAR 40-Year Reanalysis Project. *Bull. Amer. Meteor. Soc.,* **77,** 437–471.

Kanamitsu, M., W. Ebisuzaki, J. Woolen, S. K. Yang, J. Hnilo, M. Fiorino, and G. L. Potter, 2002: NCEP–DOE AMIP-II Reanalysis (R-2). *Bull. Amer. Meteor. Soc.,* **83,** 1631–1643.

Kumar, A., and M. P. Hoerling, 1998: Specification of regional sea surface temperatures in atmospheric general circulation model simulations. *J. Geophys. Res.,* **103** (D8), 8901–8907.

Pegion, K., and B. P. Kirtman, 2008: The impact of air–sea interactions on the simulation of tropical intraseasonal variability. *J. Climate,* **21,** 6616–6635.

Reynolds, R. W., N. A. Rayner, T. M. Smoth, D. C. Stokes, and W. Wang, 2002: An improved in situ and satellite SST analysis for climate. *J. Climate,* **15,** 1609–1625.

——, T. M. Smith, C. Liu, D. B. Chelton, K. S. Casey, and M. G. Schlax, 2007: Daily high-resolution blended analyses for sea surface temperature. *J. Climate,* **20,** 5473–5496.

Rienecker, M. M., and Coauthors, 2011: MERRA: NASA's Modern-Era Retrospective Analysis for Research and Applications. *J. Climate,* **24,** 3624–3648.

Saha, S., and Coauthors, 2010: The NCEP Climate Forecast System Reanalysis. *Bull. Amer. Meteor. Soc.,* **91,** 1015–1057.

Saravanan, R., 1998: Atmospheric low-frequency variability and its relationship to midlatitude SST variability: Studies using the NCAR Climate System Model. *J. Climate,* **11,** 1386–1404.

Seo, K.-H., J.-K. E. Schemm, W. Wang, and A. Kumar, 2007: The boreal summer intraseasonal oscillation simulated in the NCEP Climate Forecast System: The effect of sea surface temperature. *Mon. Wea. Rev.,* **135,** 1807–1827.

Taylor, K. E., D. Williamson, and F. Zwiers, 2000: The sea surface temperature and sea ice concentration boundary conditions for AMIP II simulations. PCMDI Rep. 60, 20 pp. [Available from National Technical Information Service, 5285 Port Royal Rd., Springfield, VA 22161.]

Woolnough, S. J., J. M. Slingo, and B. J. Hoskins, 2000: The relationship between convection and sea surface temperature on intraseasonal timescales. *J. Climate,* **13,** 2086–2104.

Wu, M. L. C., S. Schubert, I. S. Kang, and D. E. Waliser, 2002: Forced and free intraseasonal variability over the South Asian Monsoon region simulated by 10 AGCMs. *J. Climate,* **15,** 2862–2880.

Wu, R., B. P. Kirtman, and K. Pegion, 2006: Local air–sea relationship in observations and model simulations. *J. Climate,* **19,** 4914–4932.

——, ——, and ——, 2008: Local rainfall–SST relationship on subseasonal time scales in satellite observations and CFS. *Geophys. Res. Lett.,* **35,** L22706, doi:10.1029/2008GL035883.